

Magnetic two-dimensional van der Waals materials for spintronic devices

Yu Zhang(张雨), Hongjun Xu(许洪军), Jiafeng Feng(丰家峰), Hao Wu(吴昊), Guoqiang Yu(于国强), and Xiufeng Han(韩秀峰)

Citation: Chin. Phys. B, 2021, 30 (**11**): 118504. DOI: 10.1088/1674-1056/ac2808
Journal homepage: http://cpb.iphy.ac.cn; http://iopscience.iop.org/cpb

What follows is a list of articles you may be interested in

RF magnetron sputtering induced the perpendicular magnetic anisotropy modification in Pt/Co based multilayers

Runze Li(李润泽), Yucai Li(李予才), Yu Sheng(盛宇), and Kaiyou Wang(王开友)
Chin. Phys. B, 2021, 30 (**2**): 028506. DOI: 10.1088/1674-1056/abcf9d

Defect induced room-temperature ferromagnetism and enhanced photocatalytic activity in Ni-doped ZnO synthesized by electrodeposition

Deepika, Raju Kumar, Ritesh Kumar, Kamdeo Prasad Yadav, Pratyush Vaibhav, Seema Sharma, Rakesh Kumar Singh, and Santosh Kumar†
Chin. Phys. B, 2020, 29 (**10**): 108503. DOI: 10.1088/1674-1056/ab9c0c

Room-temperature electric control of exchange bias effect in $CoO_{1-\delta}$/Co films using $Pb(Mg_{1/3}Nb_{2/3})_{0.7}Ti_{0.3}O_3$ (110) substrates

Xin Wen(闻馨), Rui Wu(吴锐), Wen-Yun Yang(杨文云), Chang-Sheng Wang(王常生), Shun-Quan Liu(刘顺荃), Jing-Zhi Han(韩景智), Jin-Bo Yang(杨金波)
Chin. Phys. B, 2020, 29 (**9**): 098503. DOI: 10.1088/1674-1056/aba611

Perpendicular magnetization switching by large spin—orbit torques from sputtered Bi_2Te_3

Zhenyi Zheng(郑臻益), Yue Zhang(张悦), Daoqian Zhu(朱道乾), Kun Zhang(张昆), Xueqiang Feng(冯学强), Yu He(何宇), Lei Chen(陈磊), Zhizhong Zhang(张志仲), Dijun Liu(刘迪军), Youguang Zhang(张有光), Pedram Khalili Amiri, Weisheng Zhao(赵巍胜)
Chin. Phys. B, 2020, 29 (**7**): 078505. DOI: 10.1088/1674-1056/ab9439

Recent progress in perpendicularly magnetized Mn-based binary alloy films

Zhu Li-Jun, Nie Shuai-Hua, Zhao Jian-Hua
Chin. Phys. B, 2013, 22 (**11**): 118505. DOI: 10.1088/1674-1056/22/11/118505

TOPICAL REVIEW — Two-dimensional magnetic materials and devices

Magnetic two-dimensional van der Waals materials for spintronic devices*

Yu Zhang(张雨)[1,2], Hongjun Xu(许洪军)[1,3], Jiafeng Feng(丰家峰)[1,2], Hao Wu(吴昊)[3,†], Guoqiang Yu(于国强)[1,2,3,‡], and Xiufeng Han(韩秀峰)[1,2,3]

[1] Beijing National Laboratory for Condensed Matter Physics, Institute of Physics, Chinese Academy of Sciences, Beijing 100190, China
[2] Center of Materials Science and Optoelectronics Engineering, University of Chinese Academy of Sciences, Beijing 100049, China
[3] Songshan Lake Materials Laboratory, Dongguan 523808, China

(Received 15 July 2021; revised manuscript received 15 September 2021; accepted manuscript online 18 September 2021)

Magnetic two-dimensional (2D) van der Waals (vdWs) materials and their heterostructures attract increasing attention in the spintronics community due to their various degrees of freedom such as spin, charge, and energy valley, which may stimulate potential applications in the field of low-power and high-speed spintronic devices in the future. This review begins with introducing the long-range magnetic order in 2D vdWs materials and the recent progress of tunning their properties by electrostatic doping and stress. Next, the proximity-effect, current-induced magnetization switching, and the related spintronic devices (such as magnetic tunnel junctions and spin valves) based on magnetic 2D vdWs materials are presented. Finally, the development trend of magnetic 2D vdWs materials is discussed. This review provides comprehensive understandings for the development of novel spintronic applications based on magnetic 2D vdWs materials.

Keywords: magnetic two-dimensional van der Waals materials, spintronic devices

PACS: 85.75.–d **DOI:** 10.1088/1674-1056/ac2808

1. Introduction

Two-dimensional (2D) van der Waals (vdWs) material refers to a layered system, where a single atomic layer or several atomic layers are stacked by vdWs force bonding. The research field of 2D materials has grown rapidly since the successful exfoliation of the single-layer graphene in 2004.[1] The intriguing properties of graphene have inspired researchers from different research areas to explore the emerging phenomena in the 2D systems, and, to date, huge amounts of novel 2D vdWs materials have been proposed and discovered. The 2D vdWs materials have also attracted special attention from the spintronics community due to their prominent properties of 2D spin transport. For example, graphene-like materials that consist of light elements have a long spin lifetime and a long spin diffusion length, which make them a perfect spin transport medium. The transition metal dichalcogenides (TMDs) with strong spin–orbit coupling serve as a new platform for spin–charge interconversion and interplay with other pseudo spins (like valley spintronics). Moreover, integrating 2D vdWs materials into spintronic devices allows adding exotic functionalities, such as the gate-, pressure-, and strain-tunability,[2–7] mechanical flexibility,[8] and even new functionalities, i.e., stacking order or twist angle-dependent properties.[9–11] Although there have been many types of 2D vdWs materials, including semiconductors, metals, insulators, superconductors, and topological insulators, one of the most critical pieces of the jigsaw puzzle, i.e., the intrinsic long-range magnetism, was still missing before 2016.

According to the Mermin–Wagner theorem,[12] the long-range magnetic order is dynamically unstable in the 2D limits. It was predicted that the strong thermal fluctuations inhibit the long-range magnetic order by exciting spin waves. Fortunately, a magnetic anisotropy can induce an energy gap for the spin wave in low dimensional systems and thus forbid the spin wave excitation, which allows stabilizing the long-range magnetic order in the 2D materials.[13] In 2016, the first evidence of the stable atomically-thin magnetic vdWs material was revealed by the Raman spectrum in $FePS_3$ crystals.[14,15] Subsequently, Gong *et al.* and Huang *et al.* found the direct evidence of spontaneous magnetization in single-layer $Cr_2Ge_2Te_6$ and CrI_3 by magneto-optic Kerr effect (MOKE), respectively.[13,16] The experimental results of $Cr_2Ge_2Te_6$ and CrI_3 support the intrinsic long-range magnetic order in the vdWs systems at the 2D limit. Since then, a great number of magnetic vdWs materials, including ferromagnetic (FM) and antiferromagnetic (AFM) materials, have been studied from both *ab initio* calculations and the experiments. The typical 2D FM materials include $Cr_2X_2Te_6$ (X = Si, Ge, Sn),[13,17,18] Fe_xGeTe_2 ($x = 3, 4, 5$),[2,19–21] $CrBr_3$,[22] 1T-CrX_2 (X = S, Se, Te),[23–27] MX_2 (M = Mn, V; X = Se, Te),[28–31] $PtSe_2$,[32,33] etc.; the typical 2D AFM materials include CrX_3 (X = Cl, I),[16,34] MPS_3 (M = Cr, Ni, Fe, Mn),[14,35,36] $MnBi_2Te_4$,[37] etc.

*Project supported by the National Key Research and Development Program of China (Grant No. 2017YFA0206200), the National Natural Science Foundation of China (Grant No. 11874409), the Beijing Natural Science Foundation, China (Grant No. Z190009), the Science Center of the National Science Foundation of China (Grant No. 52088101), and the K. C. Wong Education Foundation (Grant No. GJTD-2019-14).

†Corresponding author. E-mail: wuhaoiphy@gmail.com
‡Corresponding author. E-mail: guoqiangyu@iphy.ac.cn

© 2021 Chinese Physical Society and IOP Publishing Ltd

Table 1. Representative vdWs magnetic materials which have been demonstrated in experiments.

Magnetic states	Chalcogenides	Dihalides	Trihalides
Ferromagnetic	$CrXTe_3$ (X = Si/Ge) [Cr^{3+} ($3d^3$)], Fe_xGeTe_2 (X = 3, 4, 5), 1T-$CrTe_2$, $CrSe_2$, CrS_2, $MnSe_2$, VSe_2, $PtSe_2$, Cu_2MoS_4, K_2CuF_4 etc.		$CrBr_3$ [Cr^{3+} ($3d^3$)], VI_3
	Fe_xTaS_2 (Fe intercalated)		
Antiferromagnetic (A-type)	$MnBi_2Te_4$ [Mn^{2+} ($3d^5$)] $V_{1/3}NbS_2$, $V_{1/3}TaS_2$	FeX_2 (X = Cl/Br) [Fe^{2+} ($3d^6$)]	CrX_3 (X = Cl/I) [Cr^{3+} ($3d^3$)], CrSBr
Antiferromagntic (C-type and G-type)	$MnPX_3$ (X = S/Se) (AF-Néel) [Mn^{2+}($3d^5$)]		CrOCl
	MPS_3 (M = Fe/Co/Ni) (AF-zigzag) [Fe^{2+} ($3d^6$), Co^{2+} ($3d^7$) and Ni^{2+} ($3d^8$)]		
Helimagnets	$Cr_{1/3}NbS_2$	NiX_2 (X = Br/I) [Ni^{2+} ($3d^8$)]	
		MnI_2 and CoI_2 [Mn^{2+} ($3d^5$), Co^{2+} ($3d^7$)]	
Magnetoelectrics, magnetoelastic and multiferroics	$MnPX_3$ (X= S/Se), $CuCrP_2S_6$ (magnetoelectrics) β'-In_2Se_3 (magnetoelastic)	FeX_2 (X = Cl/Br) (magnetoelectrics)	$CrCl_3$ (magnetoelectrics)
		NiX_2 (X = Br/I) (multiferroics)	
		MnI_2 and CoI_2 (multiferroics)	
Frustrated magnets		VX_2 (X = Cl/Br) [V^{2+} ($3d^3$)]	$RuCl_3$ [Ru^{3+} ($4d^5$)]

Moreover, other complex magnetic structures, such as helical magnetism,[38] topological magnetic structure, multiferroics, spin glass, and frustrated magnetism, have also been reported in the 2D vdWs systems, enriching the family of the magnetic vdWs systems. The representative magnetic vdWs materials, which have been demonstrated in experiments, are summarized in Table 1.[20,21,23,26–29,33,39–49] It is worth mentioning that, in addition to the intrinsic magnetism, orbital magnetism was also reported in some nonmagnetic TMD materials. Son *et al*. demonstrated that monolayer MoS_2 can generate valley orbital magnetization under an in-plane electric field due to the symmetry broken induced Berry curvature dipole.[50] Subsequently, Qin *et al*. realized orbital magnetization in monolayer WSe_2 via applying uniaxial strain and electric field.[51]

There are several methods for preparing 2D magnetic materials, such as growing single-crystal bulk materials combining with mechanical exfoliation to obtain atomically thin flakes, molecular-beam epitaxy (MBE), and chemical vapor deposition (CVD). These methods can be divided into two categories: top to down methods and bottom to up methods. The mechanical exfoliation method was initially used to obtain 2D magnetic vdWs materials by taking advantage of the weak vdWs force between layers.[13,16] Fei *et al*.[19] further adopted the Au-assisted mechanical exfoliation method to obtain thinner and larger Fe_3GeTe_2 crystals. Deng *et al*.[2] further developed this method by changing Au into Al_2O_3, and obtained monolayer Fe_3GeTe_2. Nevertheless, the traditional mechanical exfoliation method is very difficult to obtain large-area thin 2D magnetic materials, which limits the application of 2D magnetic materials. The MBE and CVD have also been adopted to grow 2D magnetic materials on a large scale. For example, monolayer Fe_3GeTe_2 and Cr_2Te_3 can be synthesized by using the MBE method.[52,53] At the same time, Cr_2Te_3, Cr_2S_3, and other materials were also synthesized by the CVD method.[54,55]

The discovery of magnetic vdWs materials seamlessly introduces a spin degree of freedom to conventional vdWs materials, which provides new material options for the development of spintronic devices. It is of importance to look back to the progress in this emerging research area and give an outlook to future research. We point out that there have been a few reviews, which mainly focus on the study of magnetic properties of 2D materials.[8,39,56–58] In this review, we provide an overview of recent experimental progress on the 2D magnetic materials and focus more on their applications in spintronic devices. This review includes three parts. In the first part, we focus on recalling the studies on the control of the 2D ferromagnetism. The attempts of 2D magnetic materials in spintronic devices are then reviewed. At last, we give an outlook to the future direction in this research area.

2. Control of 2D magnetic materials

The pioneering studies on the direct observation of magnetic properties were performed on $Cr_2Ge_2Te_6$and CrI_3.[13,16] $Cr_2Ge_2Te_6$ is a vdWs FM material, and its crystal structure is shown in Fig. 1(a). The magnetism of $Cr_2Ge_2Te_6$ can be described by a 2D Heisenberg model with perpendicular magnetic anisotropy, and the Curie temperature (T_C) of the bulk material is $\sim$ 61 K. It was found that its magnetic order remains in the bilayer $Cr_2Ge_2Te_6$ with a lower T_C ($\sim$ 22 K in Fig. 1(b)). Different from $Cr_2Ge_2Te_6$, CrI_3 (crystal structure shown in Fig. 1(c)) is an A-type AFM material, which possesses the FM intralayer coupling (odd layers) and the AFM interlayer coupling (even layers). Therefore, the net magnetism of a CrI_3 flake depends on the number of layers (Fig. 1(d)). $Cr_2Ge_2Te_6$ and CrI_3 are semiconductors, and therefore their carrier concentration can be relatively easily tuned by the electric field.[59–64] More interestingly, it was found that the AFM coupling between layers of CrI_3 can be tuned through electrostatic doping.[62–64] Schematic diagram of the device is shown in Fig. 2(a) (Note that the dual-gate structure enables

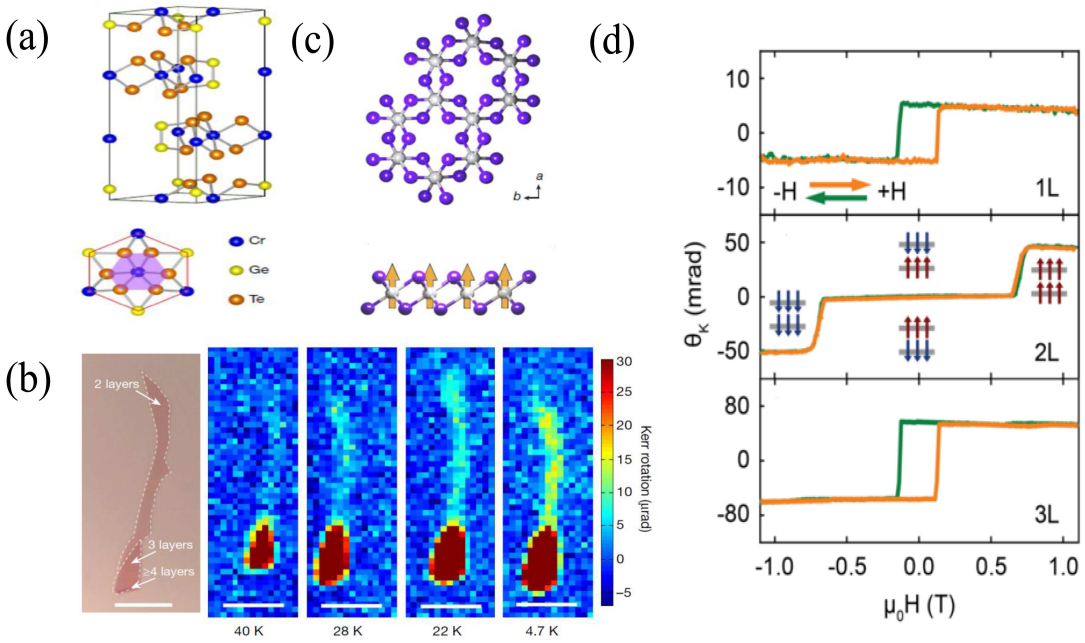


Fig. 1. (a) Crystal structure (side and top views) of $Cr_2Ge_2Te_6$. (b) Optical image of exfoliated $Cr_2Ge_2Te_6$ atomic layers and the emergence of a Kerr rotation signal for the bilayer.[13] (c) View of the in-plane (out-of-plane) atomic lattice of a single CrI_3 layer. (d) Layer-dependent magnetic ordering revealed by Kerr rotation in atomically thin CrI_3.[16] (a), (b) Reprinted with permission from Ref. [13]. Copyright 2017, Springer Nature. (c), (d) Reprinted with permission from Ref. [16]. Copyright 2017, Springer Nature.

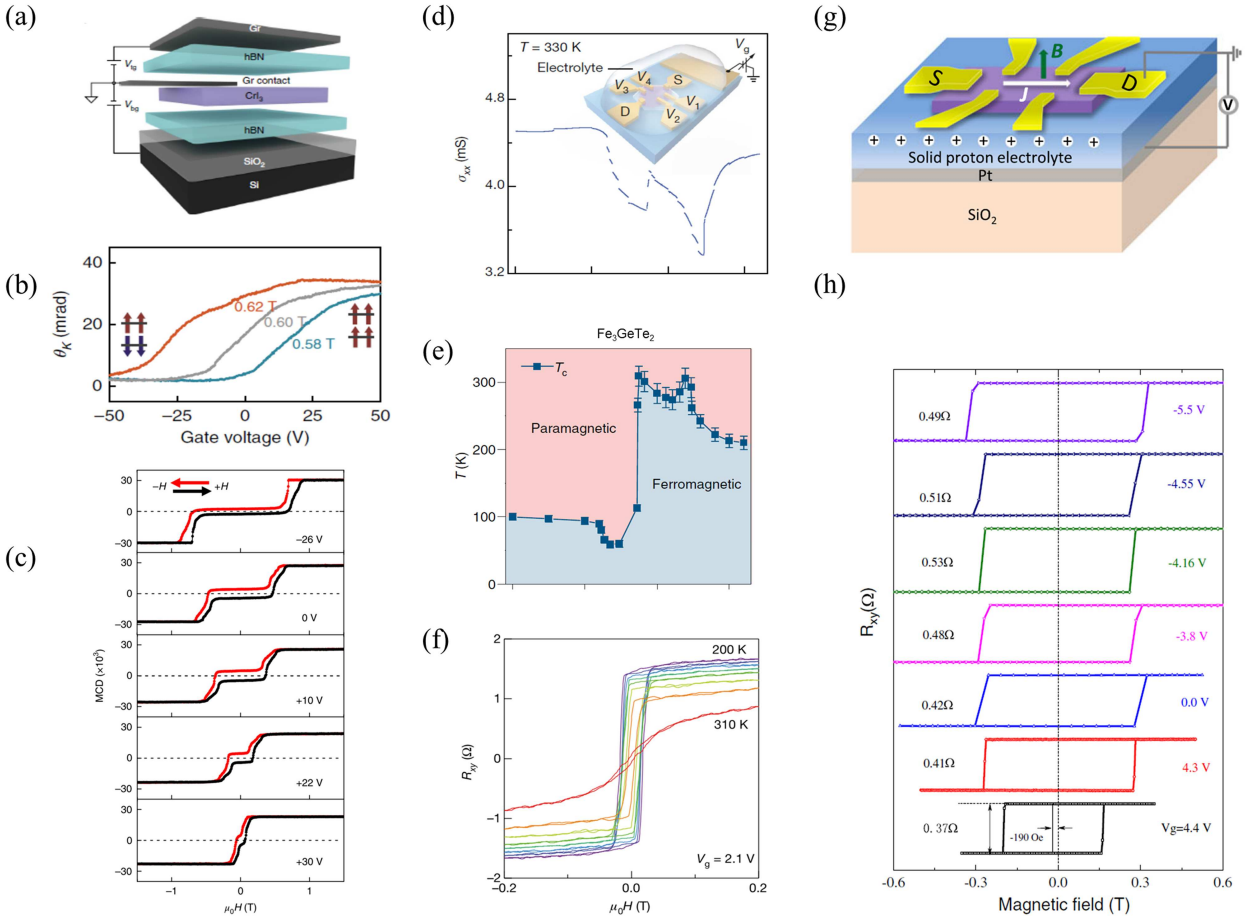


Fig. 2. (a) Schematic of a dual-gated bilayer CrI_3 device. (b) Gate-induced transition from layered AFM to FM states at different magnetic field.[62] (c) MCD versus magnetic field at 4 K at representative gate voltages.[63] (d) The schematic of the Fe_3GeTe_2 device structure and longitudinal conductance as a function of the gate voltage V_g measured in a Fe_3GeTe_2 device. (e) Phase diagram of the Fe_3GeTe_2 sample as the gate voltage and temperature are varied. (f) R_{xy} of a FGT flake under a gate voltage.[2] (g) Schematic of the Fe_3GeTe_2 Hall-bar device gated by proton. (h) Gate-tuned ferromagnetism in Fe_3GeTe_2 nanoflake.[67] (a), (b) Reprinted with permission from Ref. [62]. Copyright 2018, Springer Nature. (c) Reprinted with permission from Ref. [63]. Copyright 2018, Springer Nature. (d)–(f) Reprinted with permission from Ref. [2]. Copyright 2018, Springer Nature. (g), (h) Reprinted with permission from Ref. [67]. Copyright 2020, American Physical Society.

the electric field effect and the carrier doping effect independently). It can be seen from Figs. 2(b) and 2(c) that the mutual transformation between the AFM state and the FM state of the bilayer CrI_3 can be achieved by adjusting the gate voltage (with the assistant of an external magnetic field). In addition to conventional electrostatic doping, ionic liquid gating can significantly enhance the electric field effect and even change the transport properties of metals. Deng *et al.*[2] used the ionic liquid gating method for metallic Fe_3GeTe_2 (as shown in Fig. 2(d)), and the electron doping of about 10^{14} cm^{-2} magnitude in each layer was realized, which can increase the T_C of Fe_3GeTe_2 to room temperature. As shown in Fig. 2(f), the Fe_3GeTe_2 remains in a FM state up to 310 K after a gating voltage of 2.1 V is applied. This phenomenon was explained by the change of the density of states at the Fermi level of Fe_3GeTe_2. Compared to ionic liquid gating, the proton doping technique was developed recently, which may relieve the structure change or chemical reaction of ionic liquid gating by producing a similar doping level.[65,66] Zheng *et al.*[67] found that the proton doping produces a strong exchange coupling between adjacent layers in Fe_3GeTe_2 (see Figs. 2(g) and 2(h)). It can be seen from Fig. 2(h) that the gating voltage has a significant modulation on the coercivity field (H_c) of Fe_3GeTe_2, and a rarely seen zero-field cooled exchanged bias was achieved at the same time.

Because of the atomic thickness and the weak coupling between different layers, the structure and property of vdWs materials can be controlled by strain. Qiu *et al.* reported that patterned μm-size Fe_3GeTe_2 shows the vortex domain structure at room temperature, which was ascribed to the strain-induced effect by patterning (Figs. 3(a) and 3(b)). The authors suggested that the vortex domain structure at room temperature is induced by the finite size effect or the Ga^+ ions injection during the fabrication process.[68] Wang *et al.* realized the adjustment of coercivity and T_C of Fe_3GeTe_2 through the self-made strain test platform, as shown in Fig. 3(c). A dramatic increase of H_c by more than 150% was observed with a strain of 0.32%. Meanwhile, its T_C increased almost linearly with the stress, rising from 180 K to 210 K (Fig. 3(d)). Density functional theory calculation results suggested that a highly symmetrical Fe_3GeTe_2 bulk structure could undergo transitions with broken structural symmetries when the strain is applied, which contributes to the enhancement of T_C.[7] Besides the FM system, a strain-modulated AFM system was also reported. Ni *et al.* observed that the Néel vector could be tuned by the in-plane strain in atomically thin $MnPSe_3$.[69] As shown in Figs. 3(e) and 3(f), the Néel vector in $MnPSe_3$ is roughly along the nodal direction of the two-fold crossed pattern of the second-harmonic generation, which is controlled by the strain along different directions, e.g., 0° and 90° with respect to the x axis. In fact, in atomically thin $MnPSe_3$, the Néel vector could be rotated to any in-plane direction by the strain, which is due to the strain-locked Ising order. Song *et al.* and Li *et al.* reported the static pressure tuning of the magnetic order in the 2D magnet CrI_3.[4,5] And the interlayer coupling in CrI_3 was modulated from AFM to FM by applying a pressure of 2.7 GPa (Fig. 3(g)). In addition to the above-mentioned studies, optical injection, chemical doping, dielectric regulation, and proximity effect were also employed to tune the magnetic properties of the magnetic vdWs system, such as it has been demonstrated that magnetic vdWs materials are susceptible to external stimulus manifesting the interface engineering for structures and properties adjustments. For the atomically-thick vdWs systems, it is actually a double-edged sword that might bring controllability but lose stability at the same time.

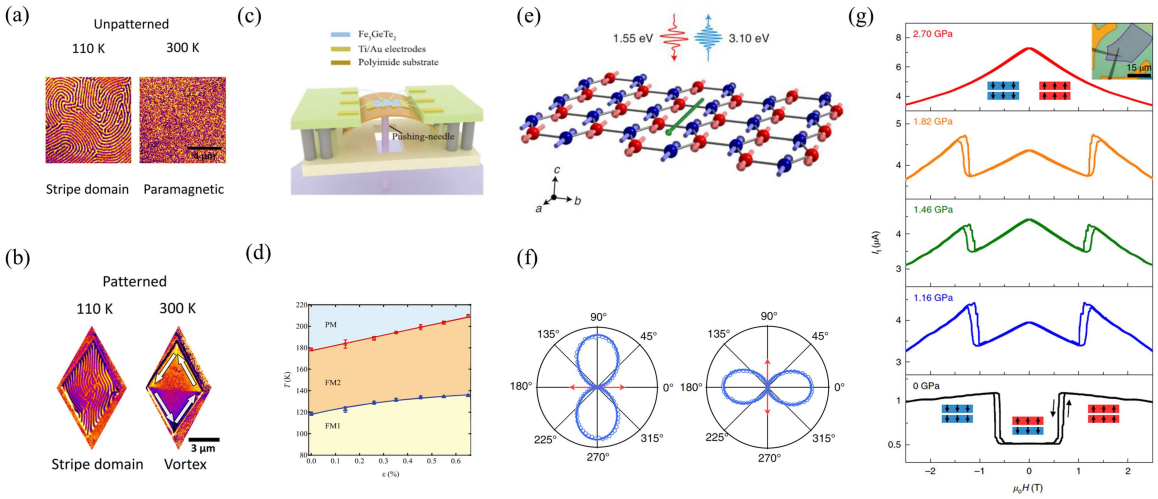


Fig. 3. (a) Enhanced T_C in Fe_3GeTe_2 and its corresponding magnetic domain structures by pattern-induced strain. (b) Schematic diagram of a device in the strain adjustment experimental.[68] (c) Phase diagram of Fe_3GeTe_2 with temperature and strain involved. (d) A schematic of the method to control the in-plane strain.[7] (e) A schematic of the in-plane AFM Néel order and second-harmonic generation measurement on $MnPSe_3$. (f) Néel vector in $MnPSe_3$, which is close to the nodal direction of the two-fold crossed pattern of second-harmonic generation, was controlled by the strain along different directions, e.g., 0° and 90° with respect to the x axis.[69] (g) Magnetization tuned by pressure.[4] (a), (b) Reprinted with permission from Ref. [68]. Copyright 2018, American Chemical Society. (c), (d) Reprinted with permission from Ref. [7]. Copyright 2020, John Wiley and Sons. (e), (f) Reprinted with permission from Ref. [69]. Copyright 2021, Springer Nature. (g) Reprinted with permission from Ref. [4]. Copyright 2019, Springer Nature.

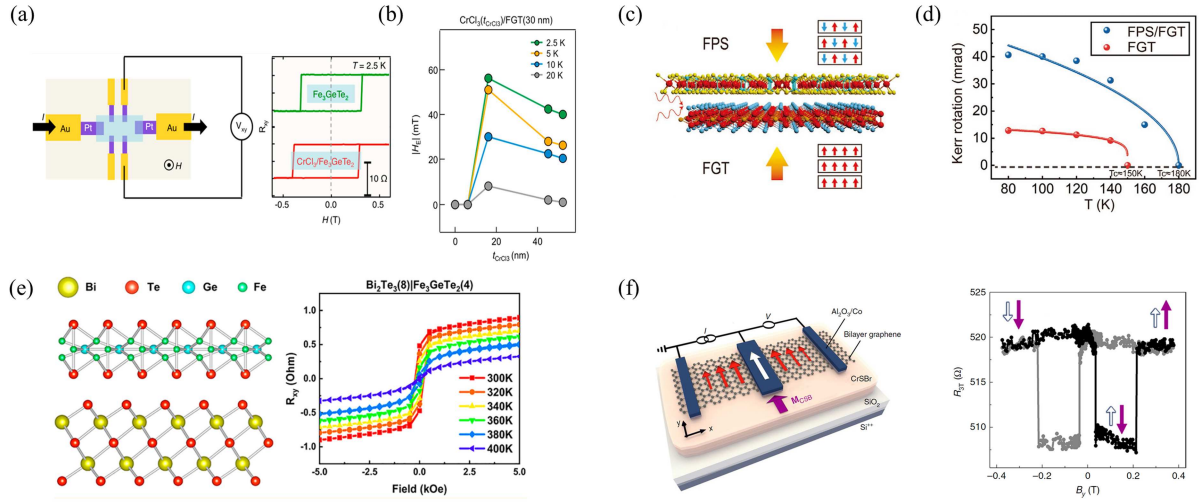


Fig. 4. (a) Emergence of exchange bias in $CrCl_3/Fe_3GeTe_2$ bilayer and (b) the exchange bias modulated by the thickness of $CrCl_3$.[70] (c) Magnetic ordering in vdWs Fe_3GeTe_2 and $FePS_3$ thin flakes; (d) extracted Kerr rotations as a function of the temperature for Fe_3GeTe_2 (red curve) and $FePS_3/Fe_3GeTe_2$ (blue curve), respectively.[73] (e) Geometric structure diagram and anomalous Hall resistance at different temperatures of Bi_2Te_3/Fe_3GeTe_2 heterostructure.[75] (f) Schematic of a three-terminal spin valve measurement geometry and independent switching of the M_{Co} and M_{CrSBr} (and so M_{Gr}) under an external magnetic field.[76] (a), (b) Reprinted with permission from Ref. [70]. Copyright 2020, American Chemical Society. (c), (d) Reprinted with permission from Ref. [73]. Copyright 2020, John Wiley and Sons. (e) Reprinted with permission from Ref. [75]. Copyright 2020, American Chemical Society. (f) Reprinted with permission from Ref. [76]. Copyright 2021, Springer Nature.

Since the layered 2D vdWs materials are binding together by the vdWs force, different (magnetic) vdWs materials can be integrated with each other without the lattice mismatching issue. Therefore, heterostructures based on (magnetic) vdWs materials provide a platform with tremendous opportunities which might emerge unique performances and novel physical mechanisms. For example, FM vdWs can be combined with various AFM materials. Zhu *et al.*[70] prepared $CrCl_3/Fe_3GeTe_2$ heterostructures, and the exchange bias-field of 50 mT at 2.5 K was achieved (Fig. 4(a)). The magnitude of exchange bias can also be modulated by the thickness of $CrCl_3$ (Fig. 4(b)). Hu *et al.*[71] used the same approach to construct the $MnPS_3/Fe_3GeTe_2$ device, in which, besides the exchange bias, they observed an anti-symmetric magnetoresistance. Zhang *et al.*[72] used vacuum exfoliation approach to prepared Fe_3GeTe_2/IrMn heterostructure, which achieved an exchange bias-field up to 895 Oe. Zhang *et al.*[73] reported the increase of T_C of Fe_3GeTe_2 from 150 K to 180 K (Fig. 4(d)) while realizing the exchange bias by utilizing the interface proximity-effect in the $Fe_3GeTe_2/FePS_3$ heterostructure (Fig. 4(c)). Interestingly, except the combination of FM material and AFM material elevates T_C, the combination of vdWs FM material with traditional AFM material achieves a similar effect. Idzuchi *et al.*[74] constructed a $Cr_2Ge_2Te_6$/NiO heterostructure with a significant increase of T_C of $Cr_2Ge_2Te_6$ after the deposition of NiO. With the thickness of NiO increasing to 50 nm, the T_C of $Cr_2Ge_2Te_6$ can reach up to 115 K, which almost doubles compared to the bare $Cr_2Ge_2Te_6$. In addition to the FM/AFM bilayer heterostructure, the heterostructure formed by magnetic vdWs materials and topological insulators (TI), graphene, and other vdWs materials also show unique properties. Wang *et al.* used MBE to grow the Bi_2Te_3/Fe_3GeTe_2 heterostructure, in which the T_C of Fe_3GeTe_2 was raised up to 400 K, which is attributed to the interfacial exchange interaction of Bi_2Te_3/Fe_3GeTe_2 (Fig. 4(e)). The author pointed out that after combining Fe_3GeTe_2 with the topological insulator Bi_2Te_3, the intralayer interactions in Fe_3GeTe_2 were dramatically increased compared to that in pure Fe_3GeTe_2 by *ab initio* calculation, which contributed to the enhanced T_C of Fe_3GeTe_2.[75] Ghiasi *et al.* fabricated a three-terminal transverse spin valve by using bilayer graphene/CrSBr heterostructure (Fig. 4(f)).[76] Here, CrSBr is a type-A AFM with much higher resistance than graphene. Surprisingly, the spin of conducting electrons in graphene became polarized ($\sim 14\%$) with the proximity effect of CrSBr, which was detected by the tunneling magnetoresistance of the junction of CrSBr/graphene/AlO_x/Co. Similarly, the proximity of CrI_3 with monolayer WSe_2 produces a large effective exchange field to WSe_2 ($\sim$ 13 T), which lifts the valley degeneracy in WSe_2 and gives rise to the polarized photoluminescence.[77] Obviously, the heterostructures-based vdWs magnetic materials serve as an ideal system for the interfacial engineering of the unique spintronic properties.

3. Application of 2D magnetic materials in spintronic devices

In the research area of spintronics, one of the major topics is the manipulation of spin via an energy-efficient and dimension-scalable manner. The electrical methods, including the electric field and current, are the promising candidates. As has been discussed above, for bilayer CrI_3, the

electrical field can change the magnetization from antiparallel coupling to parallel one and vice versa with the assistance of an external magnetic field. However, this is not a general method for controlling the magnetization of other magnetic vdWs materials. For the next-generation magnetic random-access memory (MRAM), spin–orbit torque (SOT) has been widely used for the magnetization switching by the electrical current in conventional spintronics. Therefore, for spintronic applications of the vdWs magnetic materials, manipulation of the magnetization by current-induced SOT is a crucial step.[78–80] SOT-induced switching of magnetic vdWs materials was firstly realized in the Fe_3GeTe_2/Pt bilayer device (Figs. 5(a) and 5(b)),[81,82] where the spin current injection from Pt exerts a spin torque on the magnetization of Fe_3GeTe_2 by way of spin Hall effect, and the magnetization of Fe_3GeTe_2 can be effectively controlled by the electric (spin) current polarity. As shown in Fig. 5(b), the in-plane current can switch the two states between up and down (detected by the anomalous Hall signals) with an in-plane magnetic field of 50 mT at 100 K. Note that the SOT-induced switching, in this case, is partial switching (the saturated state is marked by the dashed line in Fig. 5(b)), where the in-plane assistant magnetic field is required at the same time. Subsequently, Ostwal *et al.*[83] realized the SOT switching of $Cr_2Ge_2Te_6$ in the $Cr_2Ge_2Te_6$/Ta heterostructure (Figs. 5(c) and 5(d)). Surprisingly, the switching current density can be as low as 5×10^5 A·cm^{-2} with an in-plane magnetic field of 20 mT, which is 1–2 orders of magnitude lower than that in traditional HM/FM heterostructures, e.g., around 10^7 A·cm^{-2} for Ta/CoFeB.[79] The current-induced magnetization switching was also realized in $Cr_2Ge_2Te_6$/TI, where Mogi *et al.* fabricated a full vdWs heterostructure of $Cr_2Ge_2Te_6/(Bi_{1-x}Sb_x)_2Te_3$ bilayer by MBE and realized the current induced nearly full magnetization switching by the topological surface states (Figs. 5(e) and 5(f)).[84] Note that $Cr_2Ge_2Te_6$ is an insulator at low temperature, the switching of its magnetization by the interfacial spin injection implies the efficient spin transmission in the magnetic insulator. In addition, the magnetization was controlled by the electric current in 2D magnetic material systems with quantum anomalous Hall (QAH) effect. Serlin *et al.* found the QAH effect in twisted bilayer graphene system, which derived from the strong intrinsic interactions. It is more surprising that the switching of magnetization driven by a current of nA is realized in this system.[85,86] In addition to the FM vdWs materials, control of the magnetic order of AFM vdWs is also fascinating because of its ultrafast switching dynamics and robustness against the magnetic stray field. Current-driven AFM order switching was realized in the quasi-2D magnetic material $Fe_{1/3}NbS_2$ (Figs. 5(g) and 5(h)). It is worth noting that switching was observed at a current density as low as 2.7×10^4 A/cm^2 and the pulse duration as short as 10 μs which are orders of magnitude lower than those in the non-vdWs AFM, e.g., CuMnAs and Mn_2Au.[87–89] In this case, the AFM switching differs from FM switching in two aspects: inversion symmetry breaking in the $Fe_{1/3}NbS_2$ crystals can convert the charge current to the spin current and exert a torque on its Néel order due to the inverse spin galvanic effect; the switching behavior does not require the external magnetic field and still works under a large magnetic field up to 12 T. The SOT switching in various vdWs materials demonstrates the possibility of integrating the vdWs system into the spintronic devices for the future applications.

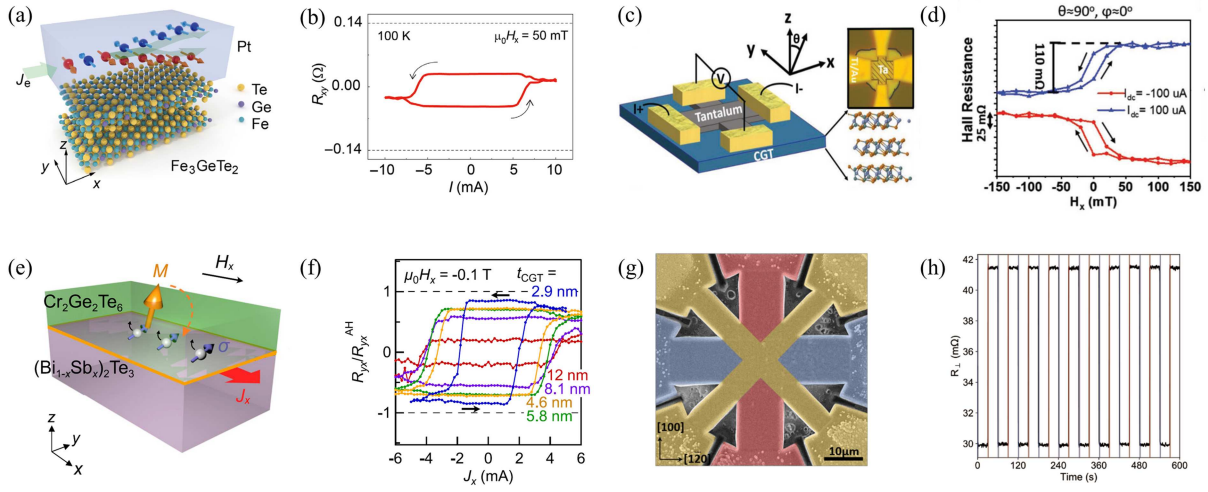


Fig. 5. Schematic view (a) and SOT-driven perpendicular magnetization switching (b) in the Fe_3GeTe_2/Pt bilayer device.[81] (c) 3D schematic and optical image of a fabricated Hall bar device from a $Cr_2Ge_2Te_6$/Ta heterostructure and measurement setup. (d) Magnetization switching of $Cr_2Ge_2Te_6$.[83] Schematic illustration of magnetization switching (e) and current-induced magnetization switching (f) in $Cr_2Ge_2Te_6/(Bi_{1-x}Sb_x)_2Te_3$ bilayer.[84] (g) A false-color SEM image of a $Fe_{1/3}NbS_2$ switching device. The transverse resistivity ($R_\perp$) is measured using the yellow contacts. A 100 μA AC probe current is applied along one yellow bar, while the voltage drop is measured along the orthogonal bar using standard lock-in techniques. Simultaneously, DC current pulses can be applied along the red and blue contacts in the [100] and [120] directions. (h) Electrical switching of $Fe_{1/3}NbS_2$.[87] (c), (d) Reprinted with permission from Ref. [83]. Copyright 2020, John Wiley and Sons. (g), (h) Reprinted with permission from Ref. [87]. Copyright 2019, Springer Nature.

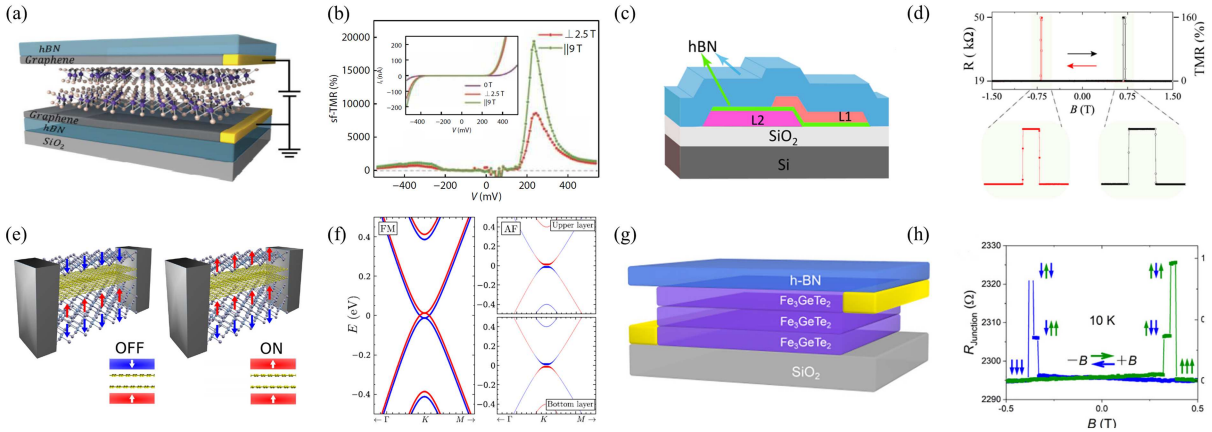


Fig. 6. (a) Schematic of 2D spin-filter magnetic tunnel junction (sf-MTJ), with bilayer CrI_3 functioning as the spin-filter sandwiched between few-layer graphene contacts. (b) Calculated sf-TMR ratio as a function of bias based on the I_t–V curves in the inset.[91] (c), (d) Schematic representation and tunneling resistance of the Fe_3GeTe_2/h-BN/Fe_3GeTe_2 spin valve.[97] (e), (f) Schematic view and band structure of a new type vdWs spin valve where a conducting 2D crystal is sandwiched between two insulating ferromagnets.[99] (g), (h) Three-state spin valves and junction resistance based on Fe_3GeTe_2.[100] (a), (b) Reprinted with permission from Ref. [91]. Copyright 2018, American Association for the Advancement of Science. (c), (d) Reprinted with permission from Ref. [97]. Copyright 2018, American Chemical Society. (e), (f) Reprinted with permission from Ref. [99]. Copyright 2018, American Physical Society. (g), (h) Reprinted with permission from Ref. [100]. Copyright 2020, Elsevier.

Magnetic tunnel junction based on the tunneling magnetoresistance (TMR) is an important criterion for MRAM due to the efficient readout signals. The first MTJ device constructed by FM vdWs was reported by Arai *et al.*, where the TMR between two relatively thick layered $Fe_{1/4}TaS_2$ flakes and amorphous TaO_x was $\sim 7\%$ at low temperature.[90] Song *et al.*[91] constructed novel spin-filter magnetic tunnel junctions (sf-MTJs) based on CrI_3 made of insulating AFM CrI_3 layers sandwiched between two graphite electrodes (Fig. 6(a)). The remarkable spin-filter tunneling magnetoresistance (sf-TMR) up to 19000% was observed in the four-layer devices, which is 1–2 orders of magnitude larger than that of conventional MgO-based MTJs (Fig. 6(b)).[92–94] This is becasue the even-layer CrI_3 with the fully AFM state is very effective for suppressing the tunneling current. Meanwhile, Klein *et al.* and Kim *et al.* observed the phenomenon in a similar structure based on CrI_3, respectively.[95,96] Wang *et al.* prepared Fe_3GeTe_2/h-BN/Fe_3GeTe_2 heterostructures by using Fe_3GeTe_2 as the FM layer and h-BN as the tunneling barrier (Fig. 6(c)). In this spin valve, TMR can reach as high as 160% at 4.2 K (Fig. 6(d)).[97] Spin valve with MoS_2 barrier has been reported as well, and the magnetoresistance of 3.1% was observed.[98] In addition, some new types of spin valves were proposed. Cardoso *et al.* predicted a spin valve based on CrI_3/graphene bilayer/CrI_3 in theory, which can show a strong magnetoresistance (Fig. 6(e)). In the antiparallel configuration, a bandgap opens at the Dirac point leading to a high-resistance off state, whereas in the parallel configuration, the graphene bilayer remains conducting (Fig. 6(f)). It provides a new scheme to generate well-defined on/off states in bilayer graphene-based spin valves.[99] Hu *et al.* proposed a homojunction based on Fe_3GeTe_2 (Fig. 6(g)). Unlike traditional spin valves, this homojunction spin valve can realize multi-state magnetic states, which can be used for multi-state storage (Fig. 6(h)).[100] These spintronic devices based on magnetic vdWs materials might pave the way for the development of spintronics to the 2D limit.

4. Conclusion and perspectives on magnetic 2D vdWs materials

In this review, the latest experimental progresses of magnetic 2D vdWs materials are reviewed towards the potential applications in spintronic devices. It shows that the manipulation of the magnetic properties of 2D vdWs materials is more diversified than conventional magnetic materials mainly because of their atomic thickness and vdWs gap. The electrical approach to control the magnetization (i.e., writing the data) of the magnetic vdWs system has been proved to be highly energy-efficient. Reading of the magnetic moments status was realized by the MTJ devices based on vdWs systems. Although the field of magnetic 2D vdWs materials is developing rapidly, there are many scientific and technical challenges for the application in spintronics: 1. How to increase the long-range magnetic order transition temperature? How to prepare 2D magnetic materials that are stable in an atmospheric environment? What is the subtle relation between the enhanced T_C and the inherent structure change? 2. How to improve magnetic stability? 3. What is the best way to control the magnetization and the spin in vdWs systems? 4. How to integrate the vdWs materials with convention spintronics? 5. How to build spintronic devices based on full vdWs stacks on a large scale? etc. Here we would like to raise some possible directions for future investigation.

1. Explore novel magnetic 2D vdWs materials. Note that most materials in Table 1 are not studied in detail for

their layer-dependent magnetic properties. The mechanisms for high T_C or T_N are not elucidated, although many vdW systems were predicted (which also need experimental demonstrations). 2D magnetic materials which are stable under atmospheric also need exploring. It was reported that 2D magnetic materials containing oxygen element have high T_C and may have high atmospheric stability, which need more experimental exploration.[101] It is crucial to obtain stable 2D magnetic materials with high T_C for the application of 2D spintronics. The possible magnetic transitions and topological structures require further studies. These works can enrich the understanding of the relationship between the structures of magnetic 2D vdWs materials and the magnetic properties in terms of symmetry, interlayer exchange interaction, magnetic anisotropy, and Dzyaloshinskii–Moriya interaction.

2. Investigate 2D materials with perpendicular magnetic anisotropy (PMA). The PMA materials and devices are much more suitable for scaling down devices regarding the density and energy performances for future magnetic memory applications.

3. Develop new detection methods. Probing the magnetism and dispersion relation of magnon in nanoscale with atomic thickness is challenging, especially for magnetic insulators and AFMs. The dynamical control and ultrafast relaxation of spin or magnetization in 2D vdWs systems are important phenomena that are still waiting to be discovered.

4. Discover novel physics and devices based on magnetic 2D vdWs materials and heterostructures. Note that the heterostructures based on magnetic 2D vdWs materials should be suitable for studying the interplay between the different degrees of freedom, e.g., charge, spin, valley, space confinement, twist angle, etc. Moreover, the study of quantum anomalous Hall effect, topological magnon excitation, and spin liquid in magnetic 2D vdWs materials will pave the way for the development of the next generation information devices with low-power, high-performance, and multi-functionality.

5. Fabricate room-temperature spintronic devices based on magnetic 2D vdWs materials which have stable long-range magnetic order at room temperature, together with the unique performances and relatively low manufactural cost.

References

[1] Novoselov K S, Geim A K, Morozov S V, Jiang D, Zhang Y, Dubonos S V, Grigorieva I V and Firsov A A 2004 *Science* **306** 666

[2] Deng Y J, Yu Y J, Song Y C, Zhang J Z, Wang N Z, Sun Z Y, Yi Y F, Wu Y Z, Wu S W, Zhu J Y, Wang J, Chen X H and Zhang Y B 2018 *Nature* **563** 94

[3] Sivadas N, Daniels M W, Swendsen R H, Okamoto S and Xiao D 2015 *Phys. Rev. B* **91** 235425

[4] Song T C, Fei Z Y, Yankowitz M, Lin Z, Jiang Q N, Hwangbo K, Zhang Q, Sun B S, Taniguchi T, Watanabe K, McGuire M A, Graf D, Cao T, Chu J H, Cobden D H, Dean C R, Xiao D and Xu X D 2019 *Nat. Mater.* **18** 1298

[5] Li T X, Jiang S W, Sivadas N, Wang Z F, Xu Y, Weber D, Goldberger J E, Watanabe K, Taniguchi T, Fennie C J, Fai Mak K and Shan J 2019 *Nat. Mater.* **18** 1303

[6] Li Q, Yang M M, Gong C, Chopdekar R V, N'Diaye A T, Turner J, Chen G, Scholl A, Shafer P, Arenholz E, Schmid A K, Wang S, Liu K, Gao N, Admasu A S, Cheong S W, Hwang C, Li J, Wang F, Zhang X and Qiu Z Q 2018 *Nano Lett.* **18** 5974

[7] Wang Y, Wang C, Liang S J, Ma Z C, Xu K, Liu X W, Zhang L L, Admasu A S, Cheong S W, Wang L Z, Chen M Y, Liu Z L, Cheng B, Ji W and Miao F 2020 *Adv. Mater.* **32** 2004533

[8] Gibertini M, Koperski M, Morpurgo A F and Novoselov K S 2019 *Nat. Nanotechnol.* **14** 408

[9] Avetisyan A A, Partoens B and Peeters F M 2010 *Phys. Rev. B* **81** 115432

[10] Cao Y, Fatemi V, Fang S, Watanabe K, Taniguchi T, Kaxiras E and Jarillo-Herrero P 2018 *Nature* **556** 43

[11] Shen C, Chu Y B, Wu Q S, Li N, Wang S P, Zhao Y C, Tang J, Liu J Y, Tian J P, Watanabe K, Taniguchi T, Yang R, Meng Z Y, Shi D X, Yazyev O V and Zhang G Y 2020 *Nat. Phys.* **16** 520

[12] Mermin N D and Wagner H 1966 *Phys. Rev. Lett.* **17** 1133

[13] Gong C, Li L, Li Z L, Ji H W, Stern A, Xia Y, Cao T, Bao W, Wang C Z, Wang Y, Qiu Z Q, Cava R J, Louie S G, Xia J and Zhang X 2017 *Nature* **546** 265

[14] Lee J U, Lee S, Ryoo J H, Kang S, Kim T Y, Kim P, Park C H, Park J G and Cheong H 2016 *Nano Lett.* **16** 7433

[15] Wang X Z, Du K Z, Fredrik Liu Y Y, Hu P, Zhang J, Zhang Q, Owen M H S, Lu X, Gan C K, Sengupta P, Kloc C and Xiong Q H 2016 *2D Mater.* **3** 031009

[16] Huang B, Clark G, Navarro-Moratalla E, Klein D R, Cheng R, Seyler K L, Zhong D, Schmidgall E, McGuire M A, Cobden D H, Yao W, Xiao D, Jarillo-Herrero P and Xu X D 2017 *Nature* **546** 270

[17] Siberchicot B, Jobic S, Carteaux V, Gressier P and Ouvrard G 1996 *J. Phys. Chem.* **100** 5863

[18] Zhuang H L, Xie Y, Kent P R C and Ganesh P 2015 *Phys. Rev. B* **92** 035407

[19] Fei Z Y, Huang B, Malinowski P, Wang W B, Song T C, Sanchez J, Yao W, Xiao D, Zhu X Y, May A F, Wu W, Cobden D H, Chu J H and Xu X D 2018 *Nat. Mater.* **17** 778

[20] May A F, Ovchinnikov D, Zheng Q, Hermann R, Calder S, Huang B, Fei Z Y, Liu Y H, Xu X D and McGuire M A 2019 *ACS Nano* **13** 4436

[21] Seo J, Kim D Y, An E S, Kim K, Kim G Y, Hwang S Y, Kim D W, Jang B G, Kim H, Eom G, Seo S Y, Stania R, Muntwiler M, Lee J, Watanabe K, Taniguchi T, Jo Y J, Lee J, Min B I, Jo M H, Yeom H W, Choi S Y, Shim J H and Kim J S 2020 *Sci. Adv.* **6** eaay8912

[22] Zhang Z W, Shang J Z, Jiang C Y, Rasmita A, Gao W B and Yu T 2019 *Nano Lett.* **19** 3138

[23] Habib M R, Wang S P, Wang W J, Xiao H, Obaidulla S M, Gayen A, Khan Y, Chen H Z and Xu M S 2019 *Nanoscale* **11** 20123

[24] Lei C A, Ma Y D, Zhang T, Xu X L, Huang B B and Dai Y 2020 *New J. Phys.* **22** 033002

[25] Fang C M, Bruggen C F v, Groot R A d, Wiegers G A and Haas C 1997 *J. Phys.: Condens. Matter* **9** 10173

[26] Li B, Wan Z, Wang C, Chen P, Huang B, Cheng X, Qian Q, Li J, Zhang Z W, Sun G Z, Zhao B, Ma H F, Wu R X, Wei Z M, Liu Y, Liao L, Ye Y, Huang Y, Xu X D, Duan X D, Ji W and Duan X F 2021 *Nat. Mater.* **20** 818

[27] Sun X D, Li W Y, Wang X, Sui Q, Zhang T Y, Wang Z, Liu L, Li D, Feng S, Zhong S Y, Wang H W, Bouchiat V, Nunez Regueiro M, Rougemaille N, Coraux J, Purbawati A, Hadj-Azzem A, Wang Z H, Dong B J, Wu X, Yang T, Yu G Q, Wang B W, Han Z, Han X F and Zhang Z D 2020 *Nano Res.* **13** 3358

[28] O'Hara D J, Zhu T C, Trout A H, Ahmed A S, Luo Y K, Lee C H, Brenner M R, Rajan S, Gupta J A, McComb D W and Kawakami R K 2018 *Nano Lett.* **18** 3125

[29] Bonilla M, Kolekar S, Ma Y J, Diaz H C, Kalappattil V, Das R, Eggers T, Gutierrez H R, Phan M H and Batzill M 2018 *Nat. Nanotechnol.* **13** 289

[30] Ataca C, Şahin H and Ciraci S 2012 *J. Phys. Chem. C* **116** 8983

[31] Fuh H R, Chang C R, Wang Y K, Evans R F L, Chantrell R W and Jeng H T 2016 *Sci. Rep.* **6** 32625

[32] Avsar A, Ciarrocchi A, Pizzochero M, Unuchek D, Yazyev O V and Kis A 2019 *Nat. Nanotechnol.* **14** 674

[33] Avsar A, Cheon C Y, Pizzochero M, Tripathi M, Ciarrocchi A, Yazyev O V and Kis A 2020 *Nat. Commun.* **11** 4806

[34] McGuire M A, Clark G, Kc S, Chance W M, Jellison G E, Cooper V R, Xu X D and Sales B C 2017 *Phys. Rev. Mater.* **1** 014001

[35] Chittari B L, Park Y, Lee D, Han M, MacDonald A H, Hwang E and Jung J 2016 *Phys. Rev. B* **94** 184428

[36] Kim K, Lim S Y, Lee J U, Lee S, Kim T Y, Park K, Jeon G S, Park C H, Park J G and Cheong H 2019 *Nat. Commun.* **10** 345

[37] Deng Y J, Yu Y J, Shi M Z, Guo Z X, Xu Z H, Wang J, Chen X H and Zhang Y B 2020 *Science* **367** 895

[38] Togawa Y, Koyama T, Takayanagi K, Mori S, Kousaka Y, Akimitsu J, Nishihara S, Inoue K, Ovchinnikov A S and Kishine J 2012 *Phys. Rev. Lett.* **108** 107202

[39] Mak K F, Shan J and Ralph D C 2019 *Nat. Rev. Phys.* **1** 646

[40] Freitas D C, Weht R, Sulpice A, Remenyi G, Strobel P, Gay F, Marcus J and Núñez-Regueiro M 2015 *J. Phys.: Condens. Matter* **27** 176002

[41] Lu K, Sapkota D, DeBeer-Schmitt L, Wu Y, Cao H B, Mannella N, Mandrus D, Aczel A A and MacDougall G J 2020 *Phys. Rev. Mater.* **4** 054416

[42] Telford E J, Dismukes A H, Lee K, Cheng M H, Wieteska A, Bartholomew A K, Chen Y S, Xu X D, Pasupathy A N, Zhu X Y, Dean C R and Roy X 2020 *Adv. Mater.* **32** 2003240

[43] Lai Y F, Song Z G, Wan Y, Xue M Z, Wang C S, Ye Y, Dai L, Zhang Z D, Yang W Y, Du H L and Yang J B 2019 *Nanoscale* **11** 5163

[44] Tian S J, Zhang J F, Li C H, Ying T P, Li S Y, Zhang X, Liu K and Lei H C 2019 *J. Am. Chem. Soc.* **141** 5326

[45] Xu C, Mao J F, Guo X Y, Yan S R, Chen Y C, Lo T W, Chen C S, Lei D Y, Luo X, Hao J H, Zheng C X and Zhu Y 2021 *Nat. Commun.* **12** 3665

[46] Wang L, Chepiga N, Ki D K, Li L, Li F, Zhu W, Kato Y, Ovchinnikova O S, Mila F, Martin I, Mandrus D and Morpurgo A F 2017 *Phys. Rev. Lett.* **118** 257203

[47] Zhang K, Khan R, Guo H Y, Ali I, Li X L, Lin Y X, Chen H P, Yan W S, Wu X J and Song L 2017 *Phys. Chem. Chem. Phys.* **19** 1735

[48] Togawa Y, Akashi T, Kasai H, Paterson G W, McVitie S, Kousaka Y, Shinada H, Kishine J I and Akimitsu J 2020 *J. Phys. Soc. Jpn.* **90** 014702

[49] Zhang T L, Wang Y M, Li H X, Zhong F, Shi J, Wu M H, Sun Z Y, Shen W F, Wei B, Hu W D, Liu X F, Huang L, Hu C G, Wang Z C, Jiang C B, Yang S X, Zhang Q M and Qu Z 2019 *ACS Nano* **13** 11353

[50] Son J, Kim K H, Ahn Y H, Lee H W and Lee J 2019 *Phys. Rev. Lett.* **123** 036806

[51] Qin M S, Zhu P F, Ye X G, Xu W Z, Song Z H, Liang J, Liu K H and Liao Z M 2021 *Chin. Phys. Lett.* **38** 017301

[52] Liu S S, Yuan X, Zou Y C, Sheng Y, Huang C, Zhang E Z, Ling J W, Liu Y W, Wang W Y, Zhang C, Zou J, Wang K Y and Xiu F X 2017 *npj 2D Mater. Appl.* **1** 30

[53] Li H X, Wang L J, Chen J S, Yu T, Zhou L, Qiu Y, He H T, Ye F, Sou I K and Wang G 2019 *ACS Appl. Nano Mater.* **2** 6809

[54] Wen Y, Liu Z H, Zhang Y, Xia C X, Zhai B X, Zhang X H, Zhai G H, Shen C, He P, Cheng R Q, Yin L, Yao Y Y, Getaye Sendeku M, Wang Z X, Ye X B, Liu C S, Jiang C, Shan C X, Long Y W and He J 2020 *Nano Lett.* **20** 3130

[55] Chu J W, Zhang Y, Wen Y, Qiao R X, Wu C C, He P, Yin L, Cheng R Q, Wang F, Wang Z X, Xiong J, Li Y R and He J 2019 *Nano Lett.* **19** 2154

[56] Huang P, Zhang P, Xu S G, Wang H D, Zhang X W and Zhang H 2020 *Nanoscale* **12** 2309

[57] Yao Y Y, Zhan X Y, Sendeku M G, Yu P, Dajan F T, Li N N, Wang J J, Zhu C C, Wang F, Wang Z X and He J 2021 *Nanotechnology* **32** 472001

[58] Huang B, McGuire M A, May A F, Xiao D, Jarillo-Herrero P and Xu X D 2020 *Nat. Mater.* **19** 1276

[59] Wang Z, Zhang T Y, Ding M, Dong B J, Li Y X, Chen M L, Li X X, Huang J Q, Wang H W, Zhao X T, Li Y, Li D, Jia C K, Sun L D, Guo H H, Ye Y, Sun D M, Chen Y S, Yang T, Zhang J, Ono S, Han Z and Zhang Z D 2018 *Nat. Nanotechnol.* **13** 554

[60] Verzhbitskiy I A, Kurebayashi H, Cheng H X, Zhou J, Khan S, Feng Y P and Eda G 2020 *Nat. Electron.* **3** 460

[61] Xing W Y, Chen Y Y, Odenthal P M, Zhang X, Yuan W, Su T, Song Q, Wang T Y, Zhong J N, Jia S, Xie X C, Li Y and Han W 2017 *2D Mater.* **4** 024009

[62] Huang B, Clark G, Klein D R, MacNeill D, Navarro-Moratalla E, Seyler K L, Wilson N, McGuire M A, Cobden D H, Xiao D, Yao W, Jarillo-Herrero P and Xu X D 2018 *Nat. Nanotechnol.* **13** 544

[63] Jiang S W, Li L Z, Wang Z F, Mak K F and Shan J 2018 *Nat. Nanotechnol.* **13** 549

[64] Jiang S W, Shan J and Mak K F 2018 *Nat. Mater.* **17** 406

[65] Jo M, Lee H J, Oh C, Yoon H, Jo J Y and Son J 2018 *Adv. Funct. Mater.* **28** 1802003

[66] Tan A J, Huang M, Avci C O, Büttner F, Mann M, Hu W, Mazzoli C, Wilkins S, Tuller H L and Beach G S D 2019 *Nat. Mater.* **18** 35

[67] Zheng G L, Xie W Q, Albarakati S, Algarni M, Tan C, Wang Y H, Peng J Y, Partridge J, Farrar L, Yi J B, Xiong Y M, Tian M L, Zhao Y J and Wang L 2020 *Phys. Rev. Lett.* **125** 047202

[68] Li Q, Yang M M, Gong C, Chopdekar R V, N'Diaye A T, Turner J, Chen G, Scholl A, Shafer P, Arenholz E, Schmid A K, Wang S, Liu K, Gao N, Admasu A S, Cheong S W, Hwang C, Li J, Wang F, Zhang X and Qiu Z Q 2018 *Nano Lett.* **18** 5974

[69] Ni Z L, Haglund A V, Wang H, Xu B, Bernhard C, Mandrus D G, Qian X, Mele E J, Kane C L and Wu L 2021 *Nat. Nanotechnol.* **16** 782

[70] Zhu R, Zhang W, Shen W, Wong P K J, Wang Q X, Liang Q J, Tian Z, Zhai Y, Qiu C W and Wee A T S 2020 *Nano Lett.* **20** 5030

[71] Hu G J, Zhu Y M, Xiang J X, Yang T Y, Huang M, Wang Z, Wang Z, Liu P, Zhang Y, Feng C, Hou D Z, Zhu W G, Gu M, Hsu C H, Chuang F C, Lu Y L, Xiang B and Chueh Y L 2020 *ACS Nano* **14** 12037

[72] Zhang Y, Xu H J, Yi C J, Wang X, Huang Y, Tang J, Jiang J L, He C L, Zhao M K, Ma T Y, Dong J, Guo C Y, Feng J F, Wan C H, Wei H X, Du H F, Shi Y G, Yu G Q, Zhang G Y and Han X F 2021 *Appl. Phys. Lett.* **118** 262406

[73] Zhang L M, Huang X Y, Dai H W, Wang M S, Cheng H, Tong L, Li Z, Han X T, Wang X, Ye L and Han J B 2020 *Adv. Mater.* **32** 2002032

[74] Idzuchi H, Allcca A E L, Pan X C, Tanigaki K and Chen Y P 2019 *Appl. Phys. Lett.* **115** 232403

[75] Wang H Y, Liu Y J, Wu P C, Hou W J, Jiang Y H, Li X H, Pandey C, Chen D D, Yang Q, Wang H T, Wei D H, Lei N, Kang W, Wen L G, Nie T X, Zhao W S and Wang K L 2020 *ACS Nano* **14** 10045

[76] Ghiasi T S, Kaverzin A A, Dismukes A H, de Wal D K, Roy X and van Wees B J 2021 *Nat. Nanotechnol.* **16** 788

[77] Zhong D, Seyler K L, Linpeng X, Cheng R, Sivadas N, Huang B, Schmidgall E, Taniguchi T, Watanabe K, McGuire M A, Yao W, Xiao D, Fu K M C and Xu X D 2017 *Sci. Adv.* **3** e1603113

[78] Miron I M, Garello K, Gaudin G, Zermatten P J, Costache M V, Auffret S, Bandiera S, Rodmacq B, Schuhl A and Gambardella P 2011 *Nature* **476** 189

[79] Liu L Q, Pai C F, Li Y, Tseng H W, Ralph D C and Buhrman R A 2012 *Science* **336** 555

[80] Yu G Q, Upadhyaya P, Fan Y B, Alzate J G, Jiang W J, Wong K L, Takei S, Bender S A, Chang L T, Jiang Y, Lang M R, Tang J S, Wang Y, Tserkovnyak Y, Amiri P K and Wang K L 2014 *Nat. Nanotechnol.* **9** 548

[81] Wang X, Tang J, Xia X X, He C L, Zhang J W, Liu Y Z, Wan C H, Fang C, Guo C Y, Yang W L, Guang Y, Zhang X M, Xu H J, Wei J W, Liao M Z, Lu X B, Feng J F, Li X X, Peng Y, Wei H X, Yang R, Shi D X, Zhang X X, Han Z, Zhang Z D, Zhang G Y, Yu G Q and Han X F 2019 *Sci. Adv.* **5** eaaw8904

[82] Alghamdi M, Lohmann M, Li J X, Jothi P R, Shao Q M, Aldosary M, Su T, Fokwa B P T and Shi J 2019 *Nano Lett.* **19** 4400

[83] Ostwal V, Shen T T and Appenzeller J 2020 *Adv. Mater.* **32** 1906021

[84] Mogi M, Yasuda K, Fujimura R, Yoshimi R, Ogawa N, Tsukazaki A, Kawamura M, Takahashi K S, Kawasaki M and Tokura Y 2021 *Nat. Commun.* **12** 1404

[85] Serlin M, Tschirhart C L, Polshyn H, Zhang Y, Zhu J, Watanabe K, Taniguchi T, Balents L and Young A F 2020 *Science* **367** 900

[86] Polshyn H, Zhu J, Kumar M A, Zhang Y, Yang F, Tschirhart C L, Serlin M, Watanabe K, Taniguchi T, MacDonald A H and Young A F 2020 *Nature* **588** 66

[87] Nair N L, Maniv E, John C, Doyle S, Orenstein J and Analytis J G 2020 *Nat. Mater.* **19** 153

[88] Wadley P, Howells B, Železný J, Andrews C, Hills V, Campion R P, Novák V, Olejník K, Maccherozzi F, Dhesi S S, Martin S Y, Wagner T, Wunderlich J, Freimuth F, Mokrousov Y, Kuneš J, Chauhan J S, Grzybowski M J, Rushforth A W, Edmonds K W, Gallagher B L and Jungwirth T 2016 *Science* **351** 587

[89] Bodnar S Y, Šmejkal L, Turek I, Jungwirth T, Gomonay O, Sinova J, Sapozhnik A A, Elmers H J, Kläui M and Jourdan M 2018 *Nat. Commun.* **9** 348
[90] Arai M, Moriya R, Yabuki N, Masubuchi S, Ueno K and Machida T 2015 *Appl. Phys. Lett.* **107** 103107
[91] Song T C, Cai X H, Tu M W Y, Zhang X O, Huang B, Wilson N P, Seyler K L, Zhu L, Taniguchi T, Watanabe K, McGuire M A, Cobden D H, Xiao D, Yao W and Xu X D 2018 *Science* **360** 1214
[92] Yuasa S, Nagahama T, Fukushima A, Suzuki Y and Ando K 2004 *Nat. Mater.* **3** 868
[93] Parkin S S P, Kaiser C, Panchula A, Rice P M, Hughes B, Samant M and Yang S H 2004 *Nat. Mater.* **3** 862
[94] Ikeda S, Hayakawa J, Ashizawa Y, Lee Y M, Miura K, Hasegawa H, Tsunoda M, Matsukura F and Ohno H 2008 *Appl. Phys. Lett.* **93** 082508
[95] Klein D R, MacNeill D, Lado J L, Soriano D, Navarro-Moratalla E, Watanabe K, Taniguchi T, Manni S, Canfield P, Fernández-Rossier J and Jarillo-Herrero P 2018 *Science* **360** 1218
[96] Kim H H, Yang B W, Patel T, Sfigakis F, Li C H, Tian S J, Lei H C and Tsen A W 2018 *Nano Lett.* **18** 4885
[97] Wang Z, Sapkota D, Taniguchi T, Watanabe K, Mandrus D and Morpurgo A F 2018 *Nano Lett.* **18** 4303
[98] Lin H L, Yan F G, Hu C, Lv Q S, Zhu W K, Wang Z A, Wei Z M, Chang K and Wang K Y 2020 *ACS Appl. Mater. Interfaces* **12** 43921
[99] Cardoso C, Soriano D, García-Martíez N A and Fernádez-Rossier J 2018 *Phys. Rev. Lett.* **121** 067701
[100] Hu C, Zhang D, Yan F G, Li Y C, Lv Q S, Zhu W K, Wei Z M, Chang K and Wang K Y 2020 *Sci. Bull.* **65** 1072
[101] Chen R, Luo F C, Liu Y Z, Song Y, Dong Y, Wu S, Cao J H, Yang F Y, N'Diaye A, Shafer P, Liu Y, Lou S, Huang J W, Chen X, Fang Z X, Wang Q J, Jin D F, Cheng R, Yuan H T, Birgeneau R J and Yao J 2021 *Nat. Commun.* **12** 3952